



HAL
open science

Synthesis, Characterization, and Self-Assembling Properties of New Amphiphilic Dendrons Bearing Branched TRIS-Derived Oligomers as Polar Head Groups

Stéphane Desgranges, Valentin Lacanau, Françoise Bonneté, Marine Soulié, Frédéric Bihel, Damien Bourgeois, Christiane Contino-Pépin

► **To cite this version:**

Stéphane Desgranges, Valentin Lacanau, Françoise Bonneté, Marine Soulié, Frédéric Bihel, et al.. Synthesis, Characterization, and Self-Assembling Properties of New Amphiphilic Dendrons Bearing Branched TRIS-Derived Oligomers as Polar Head Groups. *Macromolecules*, 2024, 57 (9), pp.4495-4507. 10.1021/acs.macromol.3c02388 . hal-04578834

HAL Id: hal-04578834

<https://hal.science/hal-04578834>

Submitted on 17 May 2024

HAL is a multi-disciplinary open access archive for the deposit and dissemination of scientific research documents, whether they are published or not. The documents may come from teaching and research institutions in France or abroad, or from public or private research centers.

L'archive ouverte pluridisciplinaire **HAL**, est destinée au dépôt et à la diffusion de documents scientifiques de niveau recherche, publiés ou non, émanant des établissements d'enseignement et de recherche français ou étrangers, des laboratoires publics ou privés.

19 regardless of their tree-like structure (*i.e.* generation type), length of the headgroup (DP_n) and
20 nature (hydrocarbonated or fluorinated, single or double-tail) or length of the hydrophobic
21 chains, self-assembling properties of H/F-DendriTACs are in agreement with usual trends of
22 surfactant assemblies, *e.g.*, as a function of chain length or polar head volume. Thus, thanks to
23 their great structural versatility, H/F-DendriTACs can provide highly tunable self-assembly
24 morphologies that can be adapted to specific applications.

25

26 INTRODUCTION

27 Amphiphilic molecules are ubiquitous in everyday life as they can be found in cosmetic
28 formulations,¹ food, pharmaceutical,² ink, paint, and coating industries.³⁻⁵ Bearing both
29 hydrophobic and hydrophilic parts, they exhibit interfacial activity and self-assemble into
30 supramolecular structures. The features of the latter rely on numerous factors such as the nature
31 and size of both hydrophobic and hydrophilic domains, their concentration, etc.^{2, 4} Depending
32 on the nature of their polar head, amphiphiles can be classified as ionic or nonionic, the latter
33 being of particular interest for biomedical applications as their structure does not change with
34 pH and as they mainly produce biocompatible particles.⁶ For many years our team has been
35 developing biocompatible amphiphiles called TAC-surfactants comprising a
36 Tris(hydroxymethyl)aminomethane-functionalized polyAcrylamide (TAC) backbone as a
37 nonionic polar head. Synthesized in one step by free radical telomerization of the
38 Tris(Hydroxymethyl)AcrylamidoMethane (THAM) monomer,^{7, 8} TAC-surfactants have been
39 used in a wide range of biomedical applications such as drug delivery and protein stabilization.⁹
40 ¹⁰ The use of an aliphatic hydrocarbon (H) or a fluorinated (F) tail of variable length leads to
41 H- and F-TAC surfactants respectively. In both cases the hydrophobic tail acts as a transfer
42 reagent (or telogen) during the THAM telomerization, giving rise to a linear polar head,
43 composed of a variable number of water-soluble tris(hydroxymethyl)aminomethane (TRIS)

44 units (see Figure 1). The so-called polyTRIS head is a linear oligomer, which is assumed to
45 wrap around itself and be an interesting alternative to polyethylene glycol (PEG) or to sugar-
46 based polar heads.

47 Although F- and H-TACs are easy to prepare at the gram scale their synthesis suffers from a
48 growing lack of batch-to-batch reproducibility as the intended size of the polyTRIS head
49 (average degree of polymerization (DP_n)) increases. Moreover, while for the F-TAC series the
50 DP_n is precisely assessed by ¹⁹F-NMR titration using an external reference,⁸ for H-TAC
51 analogues the DP_n is estimated by ¹H-NMR by comparing the area of the signal due to the
52 methyl group of the hydrocarbon tail with that of hydroxyl groups of TRIS units. Thereby, the
53 longer the polyTRIS moiety the lesser accurate is the DP_n estimation in that case.

54 In order to overcome these drawbacks (structural variability, polydispersity, DP_n estimation
55 for polyTRIS of high DP_n) keeping the main advantages of F- and H-TACs (high water
56 solubility arising from the polyTRIS polar head, biocompatibility, modular structure), we have
57 recently developed a new class of dendritic surfactants bearing dendronized PolyTRIS
58 oligomers of short DP_n (DP_n<15) as polar head groups.

59 Dendrimers and dendrons have drawn considerable attention because of their well-defined
60 molecular structure resulting in unique three-dimensional architecture and small hydrodynamic
61 radius.¹¹ One subclass are nonionic amphiphilic dendrons.^{12, 13} This subclass has been
62 extensively exemplified by the work of Haag et al, who developed a series of [hydrogenated or
63 fluorinated glycerol-based dendrons and studied the influence of structural features on their
64 self-assembly.](#)^{14, 15}

65 In comparison with F/H-TACs, which are linear oligomers whose structural modularity is
66 limited to the length of both polar and apolar parts, dendronization is expected to increase the
67 surface functionalization, hence the polar head volume, due to steric hindrance at the
68 hydrophilic surface.

85 Herein, we report the synthesis of two generations of Dendri-TAC surfactants, along with the
86 study of their structural features. AB₂ and AB₃ building blocks were used for the synthesis of
87 G₁ Dendri-TACs, leading to either a di- or a tri-branched polar head. G₂ Dendri-TACs were
88 synthesized using AB₂ units resulting in a tetra-cephalic polar head (See Scheme 1). The
89 influence of structural features of the surfactant on the size and number of aggregation (N_{ag}) of
90 resulting self-assembled architectures was studied by DLS and SAXS analyses.

91

92

93

94 RESULTS AND DISCUSSION

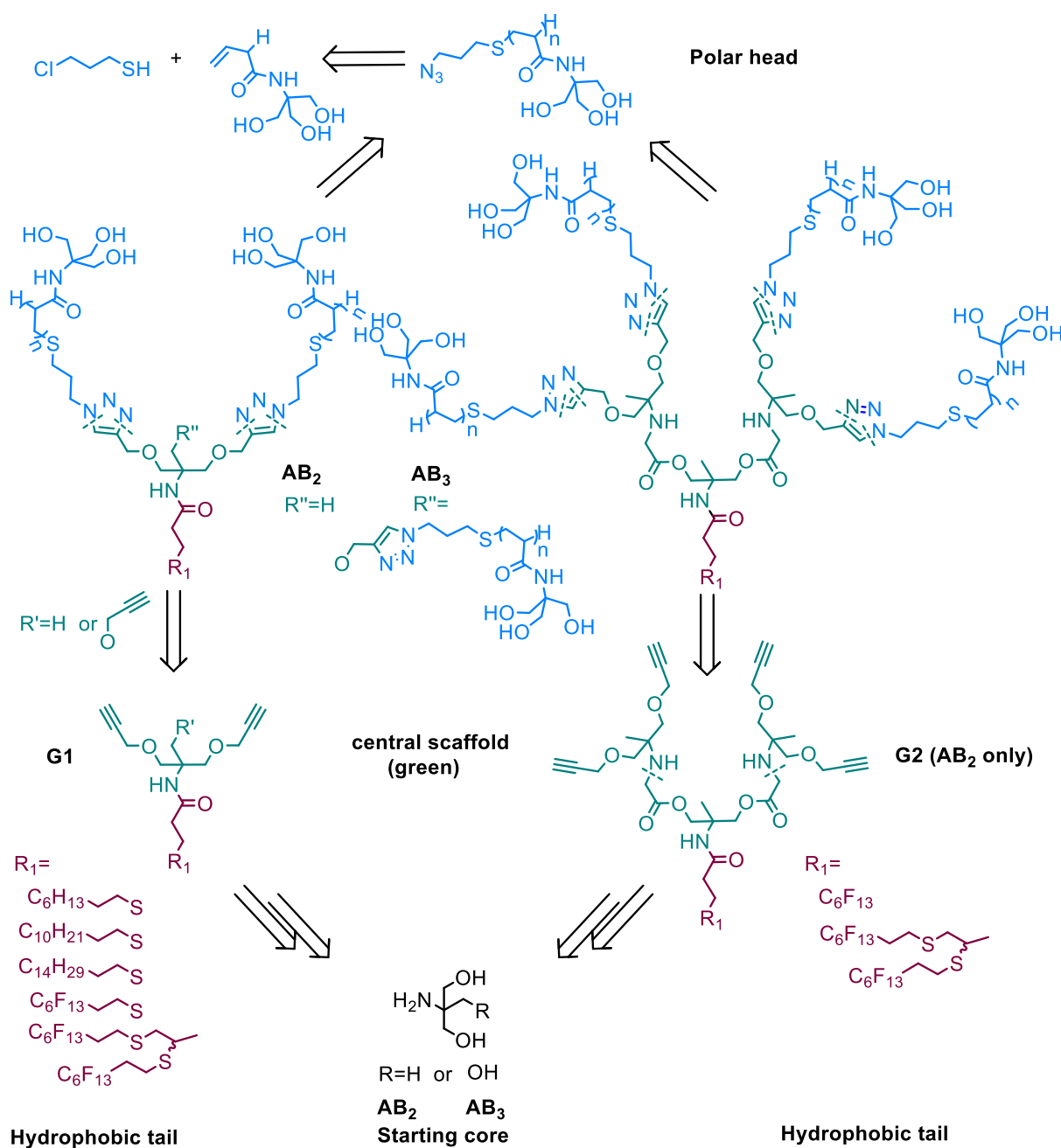
95 **Synthesis.** The Dendri-TAC surfactant family was built following a divergent synthetic
96 approach starting from a bifunctional repetitive unit (starting core) endowed on one side
97 (branching point B) with hydroxyl groups convertible to propargyl ones, in order to introduce
98 the polar head via a copper (I) catalyzed azide-alkyne cycloaddition reaction (CuAAC), and on
99 the other side (branching point A) an amino group graftable to the hydrophobic tail (HT).¹⁶
100 Retrosynthetically, the structure of Dendri-TAC molecules can be divided in 3 fragments,
101 including the HT, the central scaffold (made of AB₃ or AB₂ units) and the polar head. Each
102 functional block can be varied separately, sequentially coupled and reused to easily grow the
103 library thanks to a modular synthetic strategy (See Scheme 1). This approach allows to provide
104 a series of structurally versatile surfactants. The synthesis is based on three key steps. First, the
105 synthesis of the oligomeric polyTRIS polar head functionalized with an azido group. Secondly,
106 the modular synthesis of apolar propargyl building blocks resulting from the combination of
107 the central scaffold with the HT. Finally, the conjugation of the two former synthons through a
108 1,2,3-triazole junction after a Cu(I)-catalyzed azide-alkyne cycloaddition (CuAAC) reaction.
109 For the G₁ generation, three hydrocarbonated and two fluorinated tails of different length were

110 introduced: C_8H_{17} , $C_{12}H_{25}$, $C_{16}H_{33}$ respectively called H₈, H₁₂ and H₁₆ for the hydrocarbon
 111 series, and C_6F_{13} (single-tail) or di C_6F_{13} (double-tail) respectively called F₆ and diF₆ for the
 112 fluorinated one, with either AB₂ or AB₃ starting cores. For the G₂ generation, single- (F₆) or
 113 double-tail (diF₆) fluorinated surfactants were prepared starting from a AB₂-type core.

114

115 **Scheme 1.** Retrosynthetic pathway of Dendri-TAC surfactants

116



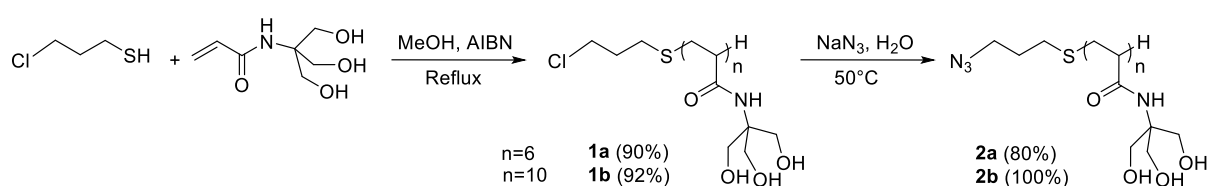
117

118

119 **Synthesis of azido-polyTRIS.** Hydrosoluble polar heads, constituted of oligomeric
120 polyTRIS moieties functionalized with azido groups, were easily synthesized in two steps. The
121 first step consists in a free radical telomerization of THAM monomer, performed in methanol
122 with chloropropanethiol as transfert agent and 2,2'-azobisisobutyronitrile (AIBN) as radical
123 initiator. Then, an azido group is introduced by nucleophilic substitution of the chlorine atom
124 in water. According to the choice of initial monomer/telogen molar ratio ($1/R_0$), the number of
125 n repeating TRIS units ($n=DP_n$) can be adjusted. Two $1/R_0$ ratios were intended namely 5 and
126 12. After a purification step by size exclusion chromatography, the resulting DP_n of azido-
127 polyTRIS oligomers were assessed by 1H -NMR, and found to be of 6 and 10 for compounds
128 **2a** and **2b** respectively (see Scheme 2). This slight drift of the DP_n values arises from the fact
129 that free radical telomerization does not offer the same level of DP_n control as living
130 polymerization techniques. However, it is a simpler, low-cost and more straightforward
131 synthetic methodology.¹⁷

132

133 **Scheme 2.** Synthetic pathway of azido-polyTRIS oligomers

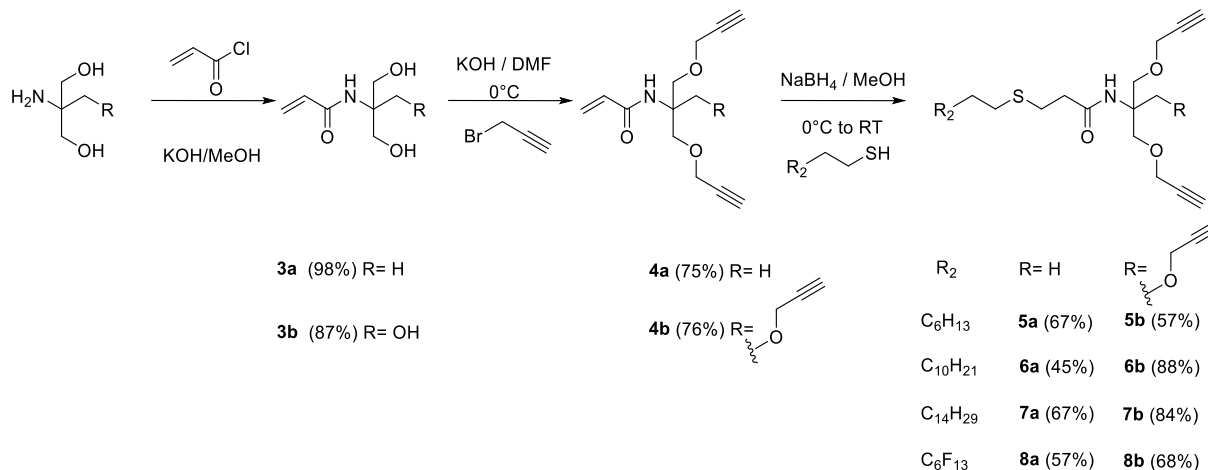


136

137 **Synthesis of apolar building blocks.** For all surfactants, the amino group of the AB_2 or AB_3
138 central scaffold is the anchor point of the HT through an amide junction. As shown in scheme
139 **3**, for single-tail analogues the amino group of the starting material (2-amino-2-methylpropane-
1,3-diol or tris(hydroxymethyl)aminomethane) was first grafted to an acryloyl moiety
140 (compounds **3a** and **3b**) followed by the propargylation of hydroxyl groups and consecutive
141 thiol-ene Michael addition of intermediates (compounds **4a** and **4b**) to commercially available

142 alkyl (C₆H₁₃SH, C₁₀H₂₁SH, C₁₄H₂₉SH) or fluoroalkyl thiols (C₆F₁₃C₂H₄SH). Apolar single tails
 143 resulting from these three steps were referred as H₈, H₁₂, H₁₆ and F₆, respectively (on
 144 compounds **5 a-b** to **8 a-b**).

145 **Scheme 3.** Synthetic pathway of single-tail apolar building blocks for G₁ DendriTACs

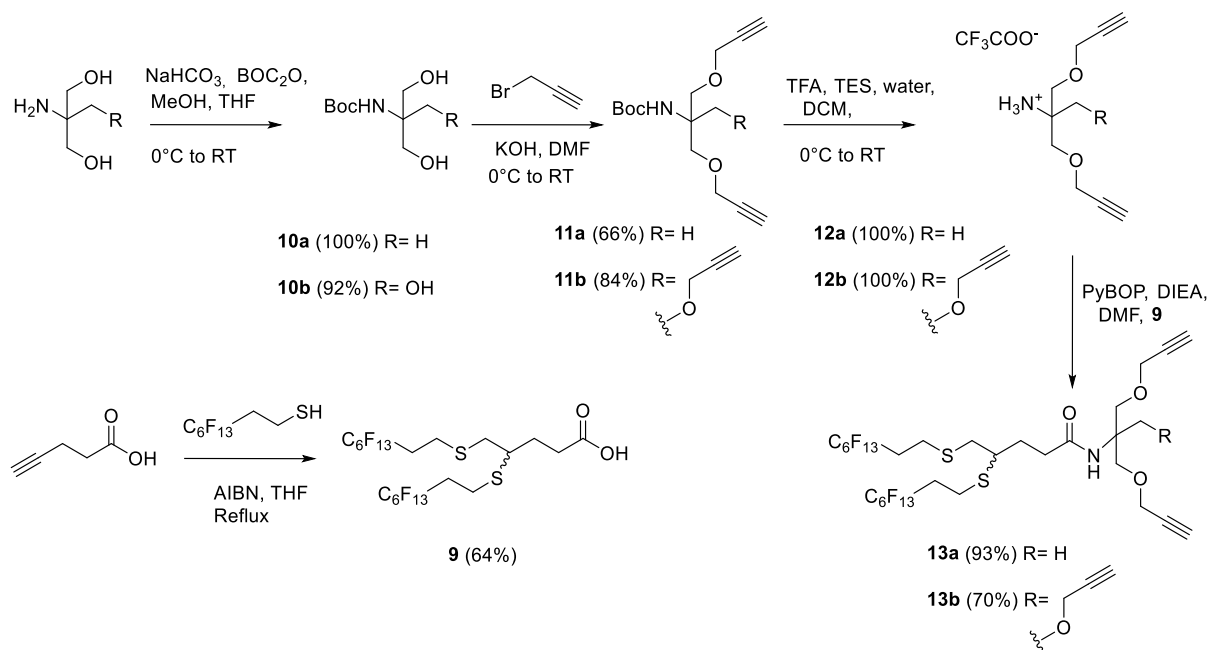


146
147

148 The synthesis of double-tail fluorinated surfactants (compounds **13a** and **13b**) is described in
 149 Scheme 4. The synthesis consists in the preparation of propargyl analogues of 2-amino-2-
 150 methylpropane-1,3-diol and of tris(hydroxymethyl)aminomethane as previously described by
 151 Chabre *et al*¹⁸ and their consecutive coupling to a double-tail acid (compound **9**) under classical
 152 conditions of peptide synthesis. The latter double-tail acid being obtained in parallel by the
 153 thiol-yne click reaction of an alkynyl carboxylic acid with an alkyl or fluoroalkyl thiol, namely
 154 4-pentynoic acid and 2-perfluorohexylethyl thiol herein. This dihydrothiolation reaction,
 155 conducted under radical conditions using AIBN, demonstrates remarkable robustness,
 156 versatility, and compatibility with a diverse range of functional groups.¹⁹

157 **Scheme 4.** Synthetic pathway of double-tail apolar building blocks for G₁ DendriTACs

158



159

160 An alternative synthetic pathway for the G1 apolar building block was also followed in order

161 to prevent thiol-yne side additions and improve the overall yield. Hence, a Michael addition

162 was first performed on compounds **3a** and **3b** before the introduction of propargyl groups, as

163 shown in scheme 5. The addition was achieved in presence of a catalytic amount of Hunig's

164 base to obtain compounds **14a** & **14b** in quantitative yield. It is noteworthy that this reaction

165 condition (methanolic N,N-Diisopropylethylamine) allowing a quantitative Michael addition

166 on **3a** and **3b** completely failed when performed on compounds **4a** and **4b**. However, lower

167 yields were obtained for the following Williamson reaction compared to the original pathway

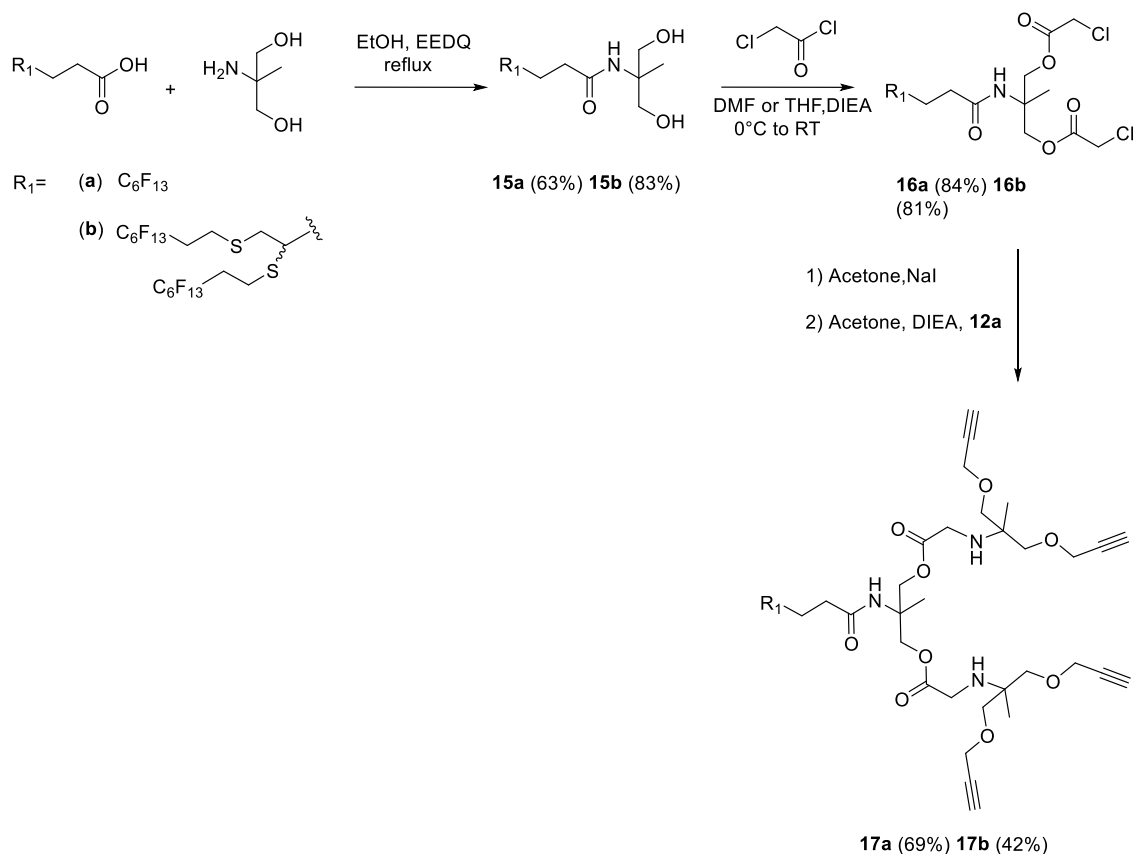
168 described on scheme 3, with 41 % & 54 % yield against 75% & 76% yield respectively. This

169 result may be due to the retro-Michael reaction that may have occurred under basic conditions

170 or prolonged reaction time.^{20, 21} Overall yields were actually close, with 43% & 52% for the

171 original pathway against 41% & 54% for the alternative pathway.

172 **Scheme 5.** Alternative synthetic pathway of G1 apolar building blocks (single-tail)



191

192

193 **Amphiphilic “click” conjugates: Coupling between the azido-polyTRIS and**

194 **propargylated apolar building blocks.** The final key step of our modular synthetic strategy

195 relied on the formation of triazole junction, employing the most widely used click method, *e.g.*

196 the Cu(I)-catalyzed azide–alkyne cycloaddition (CuAAC), to produce amphiphilic conjugates.

197 This is an attractive method for bioconjugation due to its high yields, robustness, tolerance

198 toward functional group, simple reaction conditions and generally lack of side reaction

199 occurrence.^{22, 23}

200 The click reactions between apolar building blocks **5-8**, **14**, and **17** and two azido-polyTRIS

201 analogues of different DPn (**2a** or **2b**) afforded the first and second generation of dendriTAC

202 surfactants **18-23** and **24**, respectively. Cycloadditions were carried out in a mixture of DMF

203 and water at 50°C, with a combination of copper (II) and sodium ascorbate as the source of

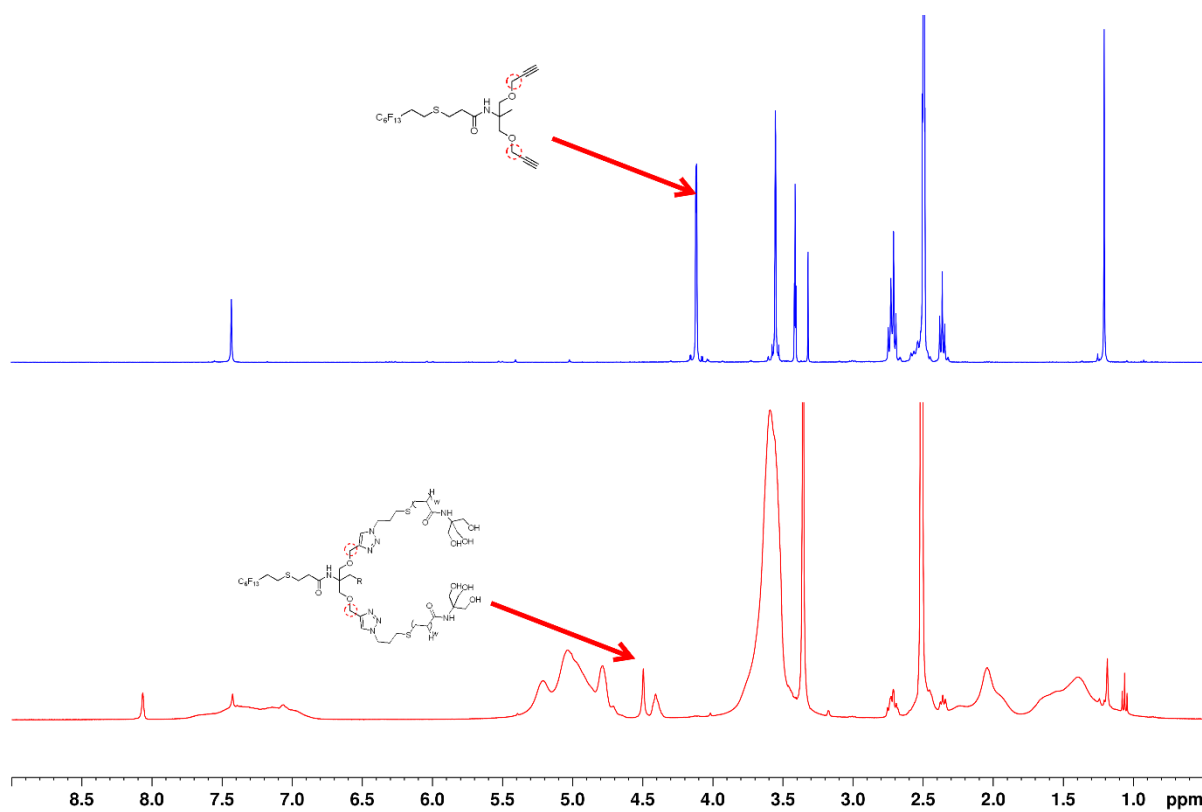
204 Cu(I) for the catalytic system. The total conversion of the alkyne to triazole was monitored by

205 ¹H-NMR, with the deshielding of the signal, assigned to the CH₂ in α position of the alkyne,

206 from $\delta = 4.12$ ppm to $\delta = 4.54$ ppm after the triazole formation (see Figure 2). Both F- and H-
207 DendriTAC surfactants were purified by size exclusion chromatography (SEC) on a Sephadex
208 LH-20 column with MeOH as eluent. The F-DendriTAC series was consecutively purified by
209 fluorosolid phase extraction (FSPE). The main impurity was the unreacted azido-polyTRIS.
210 Hence, to confirm its removal during the purification process, a 2D [1H,1H] COSY NMR
211 experiment was conducted, as signals of this unreacted azido-polyTRIS were overlapping with
212 signals from the newly formed amphiphilic click conjugates on $^1\text{H-NMR}$ spectra. The total
213 disappearance of cross peaks of coupled protons at $\delta = 1.78$ ppm, ascribed to the three
214 methylene groups of the terminal propyl chain of the azido-polyTRIS (**1a**, **2a** & **3a** in Figure 3)
215 was observed. As shown in Table 1, except for compound **20a**, purified DendriTACs showed a
216 slight increase in DP_n compared to starting azido-polar heads **2a** (DP_n = 6) or **2b** (DP_n = 10).
217 This DP_n shift can arise from the fractionation of DendriTACs, during the final LH-20
218 purification step. According to the Sephadex column features (column volume, packing...) the
219 molecular size distribution of these branched molecules can be refined compared to starting
220 linear oligomers **2a** and **2b**, thus leading to collected fractions of interest exhibiting new DP_n
221 values. It is also noteworthy that DendriTACs of low DP_n and unreacted azido-polyTRIS
222 analogues of high DP_n can coelute during the size exclusion chromatography which contributes
223 to limit some reaction yields from 20% to 70%. For the second generation, the low yields
224 obtained might be due to the ester hydrolysis that may have occurred during the coupling or
225 purification steps.

226 **Figure 2.** Click reaction monitoring. *Above:* example of $^1\text{H-NMR}$ spectrum of a fluorinated HT
227 central core. *Below:* $^1\text{H-NMR}$ spectrum of a total reaction completion.

228



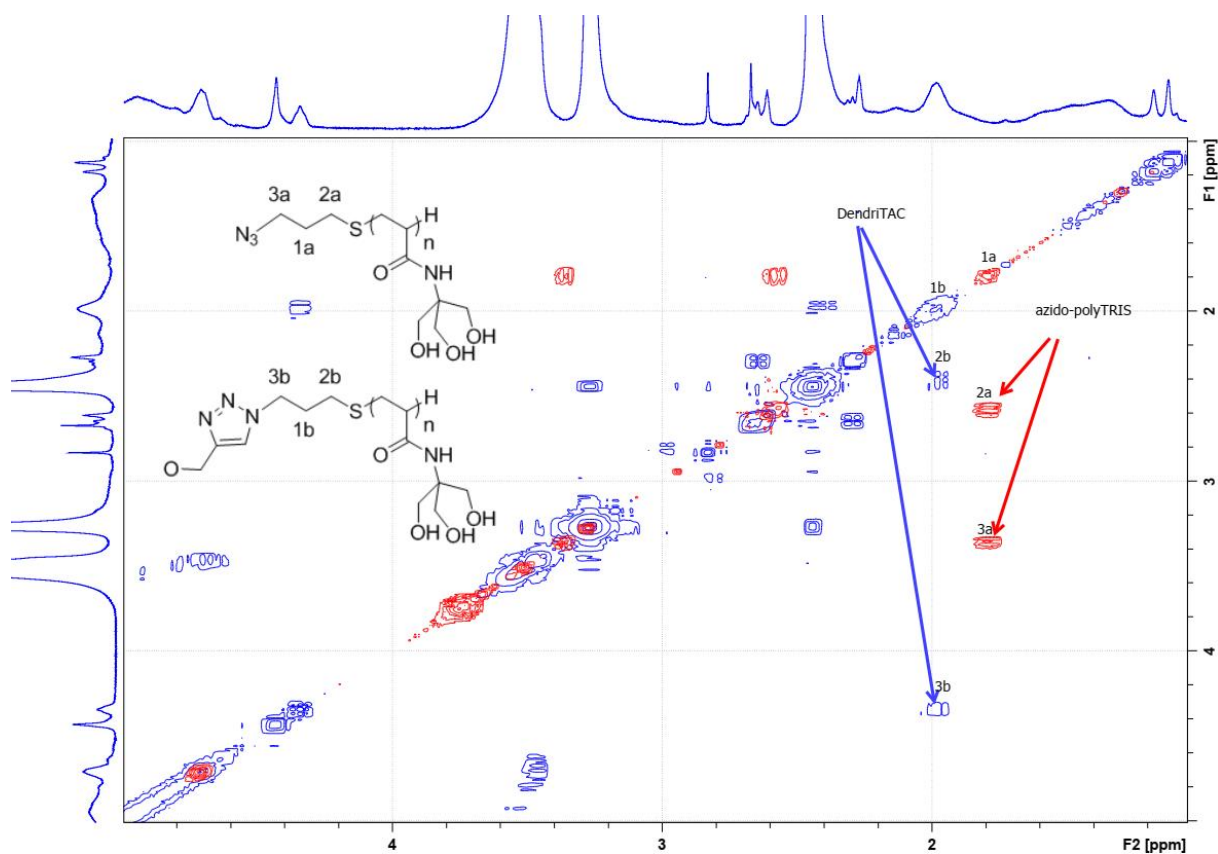
229

230 **Figure 3.** Overlay of 2D [1H,1H]-COSY NMR spectrum, in blue propargylated apolar moiety

231 spectrum and in red a DendriTAC spectrum (F₆DiTAC₆) after purification

232

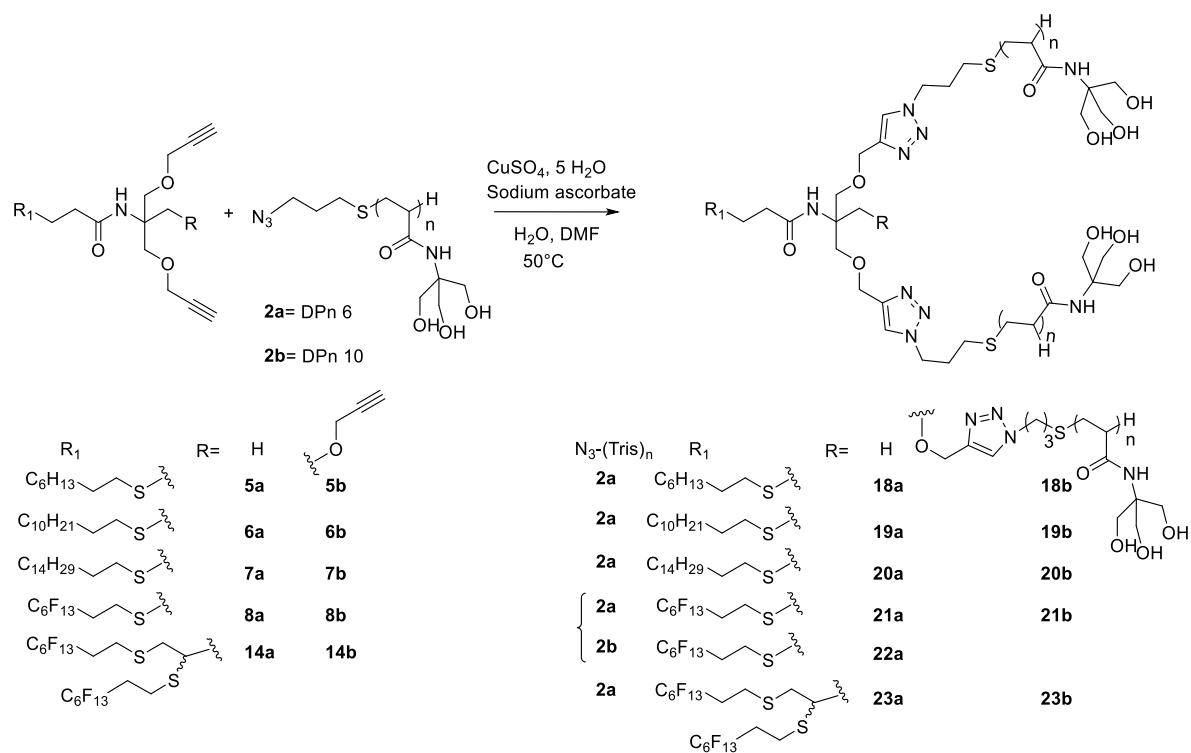
233



234

235

236 **Scheme 7.** Click reaction for G₁ DendriTAC surfactants' synthesis

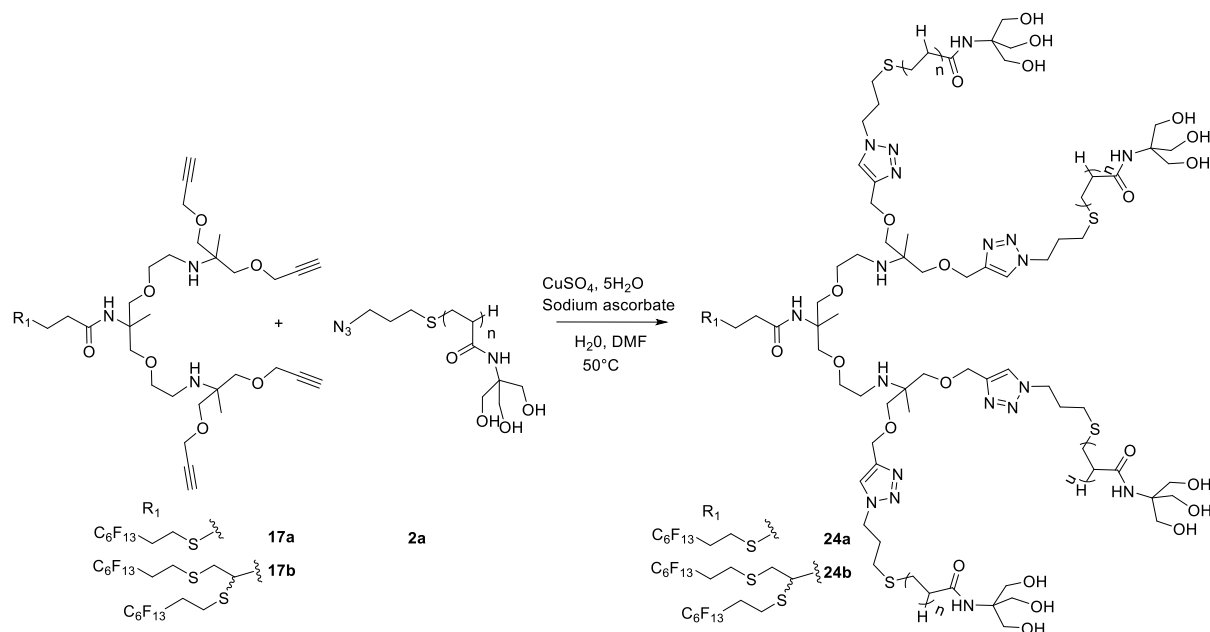


237

238

239 **Scheme 8.** Click reaction for G₂ DendriTAC surfactants' synthesis

240



241

242 **Table 1.** Surfactants' synthesis summary and characterization

G	HT¹	PH²	Ref	Yield³	DP_n	Surfactant	M_n⁴ (¹H-NMR) g/mol	M_n⁵ (GPC) g/mol	D_M⁶
G₁	5a	2a	18a	30%	9	H ₈ DiTAC ₉	3769	2170	1.11
G₁	6a	2a	19a	63%	9	H ₁₂ DiTAC ₉	3824	1940	1.11
G₁	7a	2a	20a	22%	3	H ₁₆ DiTAC ₃	1779	N/A ⁷	N/A
G₁	8a	2a	21a	20%	7	F ₆ DiTAC ₇	3301	2282	1.13
G₁	8a	2b	22a	73%	11	F ₆ DiTAC ₁₁	4702	2094	1.13
G₁	5b	2a	18b	43%	6	H ₈ TriTAC ₆	3939	2226	1.12
G₁	6b	2a	19b	41%	8	H ₁₂ TriTAC ₈	5045	1919	1.14
G₁	7b	2a	20b	29%	8	H ₁₆ TriTAC ₈	5101	1921	1.16
G₁	8b	2a	21b	65%	7	F ₆ TriTAC ₇	3296	2420	1.11
G₁	13a	2a	23a	56%	6	DiF ₆ DiTAC ₆	3357	3208	1.06
G₁	13b	2a	23b	80%	8	DiF ₆ TriTAC ₈	4403	2290	1.17
G₂	17a	2a	24a	31%	6	F ₆ TetraTAC ₆	5592	2582	1.09

G₂	17b	2a	24b	30%	6	DiF ₆ TetraTAC ₆	6058	3094	1.10
----------------------	-----	----	------------	-----	---	--	------	------	------

243 ¹ HT: hydrophobic tail; ² PH: Polar head; ³ Click reaction yield; ⁴ Number-averaged weights in
244 g/mol determined by ¹H-NMR in DMSO-d₆; ⁵ Number-averaged weights in g/mol determined
245 by GPC; ⁶ Molar Mass Dispersities ($\mathcal{D}_M = M_w/M_n$); M_n and \mathcal{D}_M were determined by DMF
246 (5mM LiBr) SEC against linear polystyrene standards. ⁷ N/A: not applicable

247 DendriTAC surfactants were analyzed by ¹H-NMR and by gel permeation chromatography
248 (GPC), number-averaged molecular weights (M_n) were determined by ¹H-NMR (M_n^4) and by
249 GPC (M_n^5) while weight-averaged molecular weights (M_w) and polydispersity (\mathcal{D}_M) were
250 assessed by GPC only. It is noteworthy that relatively narrow \mathcal{D}_M values, (comprised between
251 1.06 and 1.17) were obtained for DendriTACs (Table 1), meaning that the synthesis of azido-
252 polyTRIS series somehow occurred in a controlled manner.

253 **Self-assembly studies.** DLS and SAXS experiments have been performed to characterize
254 structural parameters, in terms of size, shape, aggregation number of this new family of
255 hydrogenated and fluorinated surfactants in aqueous solution. H/F-DendriTACs were dissolved
256 in Milli-Q water and studied as a function of surfactant concentration between 0.8 and 50
257 mg/mL to highlight changes in shape and/or intermicellar weak interactions. DLS experiments
258 were conducted prior to SAXS in order to evaluate both polydispersity (PDI) of surfactant
259 solutions and hydrodynamic radius (R_H) of surfactant assemblies in solution. The PDI values
260 of all compounds were found less than 0.2 suitable for SAXS experiments (see SI, Table S1).
261 Indeed, SAXS analyses require quite monodisperse samples for reliable results. SAXS profiles
262 are shown only at 20 or 25 mg/mL in Figure 4. SAXS patterns with concentration were
263 measured only for H-DendriTACs (see SI, Figure S4) due to the low quality of SAXS curves
264 (ratio signal/noise) for F-DendriTACs at low concentrations. For all H/F-DendriTACs, the
265 radius of gyration (R_G) was determined from the linear Guinier approximation $\ln I(q) = \ln I(0)$
266 $- (qR_G)^2/3$ at very small angles, *i.e.* such that $qR_G < 1.3$) and the maximum micelle dimension
267 (D_{max}) from the pair distribution function (PDF) by Inverse Fourier Transformation of the

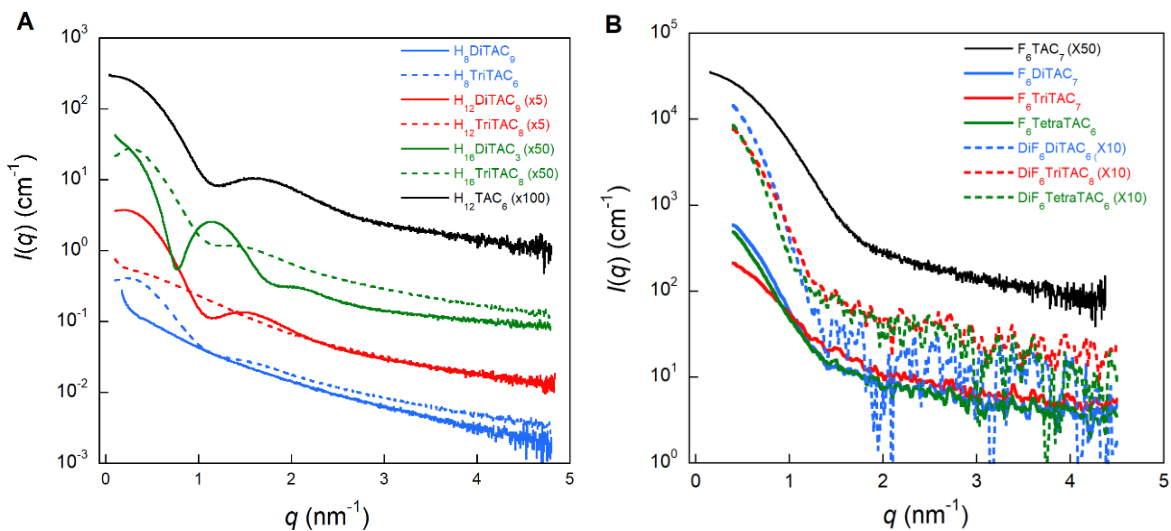
268 scattering intensity using the program GNOM²⁴ (see SI, Figure S2A). A Kratky representation
 269 (*i.e.* a plot $q^2I(q)$ as function of q) was also performed to evaluate if the assemblies were
 270 globular, flexible or non-assembled. The aggregation number N_{ag} , *i.e.* the number of surfactant
 271 molecule per surfactant assembly, was finally determined from the absolute forward intensity,
 272 $I(0)$ in cm^{-1} , *via* the expression:

$$273 \quad N_{ag} = N_a \frac{I_{\text{surf}}(0)}{M_{\text{mono}} \cdot c [r_0 \cdot v_p \cdot (\rho_{\text{surf}} - \rho_0)]^2}$$

274 with N_a the Avogadro's number, v_p the specific volume of surfactant (cm^3/g), ρ_{surf} and ρ_0 the
 275 electron scattering length densities (e^-/cm^3) of surfactant and water respectively, M_{mono} the
 276 molar mass of each surfactant monomer, r_0 the classical electron radius equal to $0.28179 \cdot 10^{-12}$
 277 cm/e^- . The partial specific volumes, v_p , were calculated from chemical composition.²⁵ All
 278 structural parameters are listed in table 2.

279

280 **Figure 4:** SAXS profiles, $I(q)$ versus q , for H-DendriTAC (A) at 25 mg/mL (H_8 -Di & TriTAC,
 281 H_{12} -Di & TriTAC) and 20 mg/mL (H_{16} -Di & TriTAC), for F-DendriTACs (B) at 20 mg/mL.
 282 (The curves are shifted for more clarity: $\times 5$, $\times 10$, $\times 50$, $\times 100$ represents offset parameter of the
 283 curve from its original position)



284

285
286
287
288

Table 2: Structural parameters of H/F-DendriTAC assemblies obtained from SAXS and DLS

289 analysis

Entry	Surfactant	DPn	Total TRIS units	R_G nm (SAXS)	D_{max} nm (SAXS)	R_H nm (DLS)	N_{ag} (SAXS)
H-DendriTACs[†]							
1	H ₈ DiTAC ₉	9	18	2.20+/-0.05	7.5+/-0.5	1.5	3
2	H ₈ TriTAC ₆	6	18	2.75+/-0.01	9.0+/-0.5	1.5	7
3	H ₁₂ DiTAC ₉	9	18	3.05+/-0.01	8.7+/-0.3	3.5	20
4	H ₁₂ TriTAC ₈	8	24	1.79+/-0.01	6.5+/-0.1	4.5	1
5	H ₁₆ DiTAC ₃	3	6	4.19+/-0.01	10.4+/-0.1	5.2	21
6	H ₁₆ TriTAC ₈	8	24	3.25+/-0.05	9.5+/-0.1	2.8	15
F-DendriTACs[‡]							
7	F ₆ DiTAC ₇	7	14	2.80+/-0.05	7.6+/-0.1	2.4	14
8	F ₆ DiTAC ₁₁	11	22	3.10+/-0.05	9.9+/-0.1	3.3	9
9	F ₆ TriTAC ₇	7	21	2.37+/-0.02	6.6+/-0.1	1.7	3
10	F ₆ TetraTAC ₆	6	24	2.72+/-0.02	7.0+/-0.1	2.8	7
11	DiF ₆ DiTAC ₆	6	12	3.50+/-0.05	9.5+/-0.5	4.6	37
12	DiF ₆ TriTAC ₈	8	24	2.75+/-0.12	8.05+/-0.1	1.2	11
13	DiF ₆ TetraTAC ₆	6	24	3.63+/-0.02	9.3+/-0.5	4.7	15
H/F-TACs[†]							
14	H ₁₂ TAC ₆	6	6	2.78+/-0.01	8.5+/-0.3	3.0	29
15	F ₆ TAC ₇	7	7	2.37+/-0.01	7.7+/-0.1	2.5	13

290 *Structural parameters for H/F-DendriTACs and H/F-TACs at 20-25 mg/mL; [†]these SAXS*
 291 *measurements were performed in a q-range of 0.032–4.93 nm⁻¹ on BM29 at ESRF; repulsive*
 292 *interactions at very small angles are clearly visible for some assemblies (entries 2, 3, 6). [‡]These*
 293 *SAXS measurements were performed in a q-range of 0.2– 4.5 nm⁻¹ on a bench-top SAXS system*
 294 *at ICSM; no specific interactions are visible in this q-range.*

295

296 From scattering experiments (Figure 4) we observe that H/F-DendriTACs form small
297 globular assemblies in water regardless of their tree-like structure (*i.e.* generation type), length
298 of the headgroup (DP_n) and nature (hydrocarbonated or fluorinated, single or double-tail) or
299 length of the hydrophobic chains. This is confirmed by the Kratky plots (See SI Figures S2B-
300 C), which highlight a globular micellar structure as seen by a bell-shaped (Gaussian) peak for
301 all H/F-DendriTACs at small q ($< 1 \text{ nm}^{-1}$), except for H₁₂TriTAC₈ and H₈DiTAC₉, which show
302 a plateau at large q typical of non-globular or flexible objects. Some SAXS curves (for
303 surfactants H₁₂TAC₆, H₁₂DiTAC₉ and H₁₆DiTAC₃ in Figure 4A) exhibit a distinct 2nd maximum
304 in the intermediate q -region, whose value is inversely proportional to a size in the micelle. This
305 peak, which is characteristic of a core-shell structure where a large difference in the scattering
306 contrast exists between the polar head group and the apolar tail, is more pronounced for H-
307 DendriTACs than for F-DendriTACs. In addition, regarding surfactants H₈TriTAC₆,
308 H₁₂DiTAC₉ and H₁₆TriTAC₈, the profile of scattering intensities recorded at small angles (*i.e.*
309 low q -region) is clearly indicative of repulsive interactions between micelles (Figure 4/A). In
310 table 2 are listed R_H , the micelle volume-weighted hydrodynamic radius determined by DLS,
311 R_G the radius of gyration and D_{max} , the maximum dimension of the DendriTAC assemblies,
312 both determined by SAXS. For all surfactants, R_H and R_G are lower than 6 nm, and D_{max} remains
313 below 11 nm. Compared to conventional surfactants,²⁶ all compounds present small aggregation
314 numbers, except DendriTAC 4 (H₁₂TriTAC₈), which is a monomer form at this concentration
315 in view of its low aggregation number ($N_{\text{ag}} = 1$). Overall, self-assembling properties are in
316 agreement with usual trends of surfactant assemblies, *e.g.*, as a function of chain length or polar
317 head volume. However, the high degree of structural versatility of H/F-DendriTACs, which
318 offers a wide range of aggregate morphologies, can be tailored to specific applications.

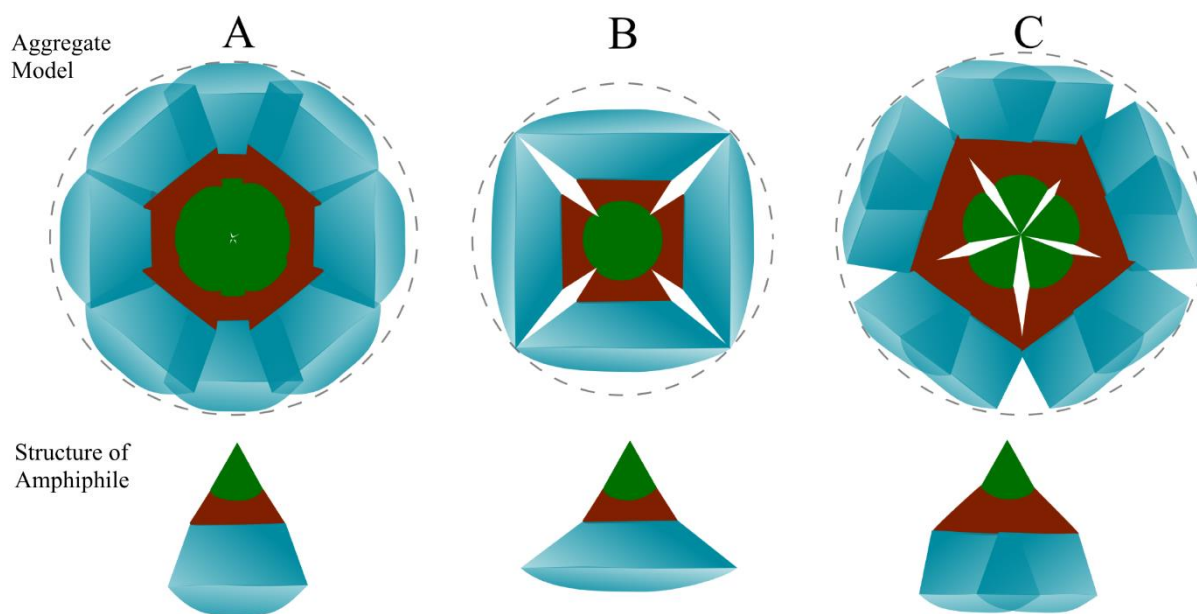
319 Regarding H-DendriTACs, for a defined headgroup, *i.e.* same length and tree-like structure
320 (*e.g.* entries 1 & 3 and 4 & 6), N_{ag} , R_G and almost all R_H values increase with the elongation of

321 the hydrophobic tail reflecting a better anchoring of monomers in the micelle due to higher
322 hydrophobic interactions between apolar chains, consistent with literature and previous
323 studies.^{27, 28} The aggregation numbers approximatively increase by 15 monomers per micellar
324 aggregates for a group of four carbons added on the hydrocarbonated tail. Whereas for the same
325 tree-like structure, this extension of the hydrophobic tail (four carbons) is balanced by a
326 reduction in the length of the headgroup, *i.e.* DPn values, and leads to an equivalent aggregation
327 number (entries **3** & **5**). For the same apolar chain, the micelle size decreases with increasing
328 total number of TRIS units (entries **3** & **4** and **5** & **6**), which is achieved by adding a polar
329 branch from AB₂ to AB₃ with either comparable (entries **3** & **4**) or higher DPn values (entries
330 **5** & **6**). This is in agreement with the concept of molecular packing parameter P (P being
331 defined as $V_o/a_e l_o$, where V_o is the surfactant tail volume, l_o is the tail length, and a_e is the
332 equilibrium area per molecule at the aggregate surface) introduced by Israelachvili et al.²⁹ The
333 addition of several hydrated TRIS units (either by elongation or branching enhancement)
334 improves the repulsion between polyTRIS branches, leading to an increase in the polar head
335 volume and therefore in the equilibrium area a_e . This induces a decrease in the packing
336 parameter P leading to the formation of smaller objects. These repulsive interactions between
337 TRIS units at the surface of surfactants also contribute to repulsive interactions between
338 micelles clearly observable on SAXS curves in the case of H₈TriTAC₆, H₁₂DiTAC₉ and
339 H₁₆TriTAC₈ (entries **2**, **3**, **6**) at very small angles (*i.e.* $q \rightarrow 0$) by a decrease in $I(q)$, which can
340 slightly underestimate R_G and forward intensity $I(0)$ thus impacting assembly size and mass
341 values. It is noteworthy that for surfactants with both identical apolar chain length and same
342 total number of TRIS units, micelle size decreases with longer polyTRIS branches (entries **1** &
343 **2**), the equilibrium area a_e due to repulsion between longer AB₂-connected branches being
344 higher than for shorter AB₃ ones.

345 In the case of fluorinated surfactants, the latter repulsion is counterbalanced by an improved
346 hydrophobic interaction between fluorinated chains, also referred as “fluorophilicity”,
347 consistent with a closely-packed fluorinated core.^{30,31} This leads to a decrease of the
348 aggregation number (entries **8** & **9**). If we compare the evolution of the structural parameters
349 from H₈DiTAC₉ to H₈TriTAC₆ (entries **1** & **2**) with those of fluorinated surfactants with the
350 same carbon atoms number on the hydrophobic tail, namely from F₆DiTAC₁₁ to F₆TriTAC₇
351 (entries **8** & **9**), the trend between size and aggregation number is clearly reversed: for H₈-
352 DendriTACs (entries **1** & **2**) it seems that the repulsion between the polar heads (due to a
353 combination of steric hindrance and strong hydration of hydroxyl groups) increases with the
354 length of the polyTRIS chains and with the easier unfolding of these chains from AB₃ to AB₂
355 branching type. Then, from H₈TriTAC₆ to H₈DiTAC₉ (entries **2** & **1**) the aggregation number
356 decreases and the size of micelles too. While for F₆-DendriTACs, both hydrophobicity and
357 lipophobicity of fluorinated chains, along with their lower conformational freedom (rigid rod-
358 like chains) concur to a “super” hydrophobic binding interaction between F-chains (mainly
359 driven by the entropic gain of water molecules in bulk water) and contribute to their ordered
360 packing into the micelle core.³⁰⁻³² Their combination to bulky oligomeric head groups, probably
361 confers a more conical shape to F-DendriTAC monomers with a more "classical" influence of
362 the tree-like structure on the volume of the heads: AB₃ induces a greater curvature of the
363 surfactant with stronger anchoring of fluorinated tails in the micelle core, resulting in smaller
364 micelles when moving from AB₂ to AB₃. The general trend observed from F₆DiTAC₁₁ to
365 F₆TriTAC₇ (entries **8** & **9**) is that both the aggregation number and the micelle size decrease
366 even though the AB₂ analogue F₆DiTAC₁₁ is endowed with longer polyTRIS branches. It is
367 interesting to note that for an equivalent total number of TRIS units (18 for the two H₈-
368 DendriTACs and 21-22 for the two F₆-DendriTACs), the impact of the “branching/elongation”
369 effect is reversed between H₈- and F₆- chains. The aggregation behavior of F-DendriTACs

370 seems to be more affected by the branched geometry of the polar head groups (R_G - R_H and N_{ag}
 371 decrease with the branching effect) compared to H-DendriTACs more affected by the
 372 elongation of polyTRIS units (R_G - R_H and N_{ag} decrease with the elongation effect).

373 **Figure 5:** A, B, C represent respectively the structure (below) and proposed aggregation
 374 model (above) for G_1/AB_2 , G_1/AB_3 , and G_2/AB_2 - AB_2 amphiphiles



375
 376 In regards to the F-DendriTACs series, they all possess the same $C_6F_{13}C_2H_4$ hydrophobic
 377 chain length, either in a single or double-tail form. Always in agreement with the concept of
 378 packing parameter, for F-DendriTACs with rather identical heads in terms of the length and
 379 number of polyTRIS branches (comparing F_6DiTAC_7 to DiF_6DiTAC_6 ; $F_6TriTAC_7$ to
 380 $DiF_6TriTAC_8$ and $F_6TetraTAC_6$ to $DiF_6TetraTAC_6$), as the volume of the hydrophobic part
 381 increases (from single to double-tailed surfactants), P increases leading to larger objects (entries
 382 7 & 11; 9 & 12; 10 & 13). In the same way, as for H-DendriTACs, the micelle size decreases
 383 with the addition of one polar branch, from AB_2 to AB_3 when polyTRIS branches have similar
 384 DP_n values (entries 7 & 9; 11 & 12, Figure 5-A&B).

385 In contrast, for a same hydrophobic tail and same branching structure, when the length of the
 386 headgroup increases from 7 to 11 TRIS units per branch (entries 7 & 8), both R_H and R_G slightly
 387 increases, whereas N_{ag} decreases. The decrease in N_{ag} can be explained by the fact that if the

388 headgroups are larger, less surfactants are required to fill the same volume. Indeed, N_{ag} is related
389 to the geometric parameters of surfactants by the expression $N_{ag} \sim (4\pi lo^2)/a_e$ (with a_e the
390 equilibrium area per molecule at the aggregate surface and lo the tail length).³³⁻³⁵ Thus, if a_e
391 increases, N_{ag} decreases. However, we cannot rule out the possibility that the shape of micelles
392 has changed as a result of the concept of molecular parameter (*vide supra*). Regarding the
393 generations G_1 and G_2 , for F-DendriTACs with a same AB_2 branching structure and close DPn
394 value per polyTRIS branch, F_6DiTAC_7 versus $F_6TetraTAC_6$ and DiF_6DiTAC_6 versus
395 $DiF_6TetraTAC_6$, little variation in the size of the assemblies is observed (R_G and R_H) although
396 for the single-tailed (entries **7 & 10**) R_H slightly increases, while N_{ag} is divided by at least 2 (see
397 entries **7 & 10, 11 & 13**). This trend is consistent with the results described previously on the
398 impact of the headgroup volume. Thus, between G_1 and G_2 series with identical apolar chains,
399 the micelle shape is retained while G_2 ones have a lower N_{ag} due to the wider/bulkier headgroup.
400 Although there is no great variation in the size of the resulting assemblies, a difference in the
401 transport properties may arise from G_1 to G_2 DendriTACs due to the volume variation of the
402 central scaffold between polyTRIS branches (Figure 5-A&C).

403 For each single- or double-tail F-DendriTACs series of generation G_1 , it is again noteworthy
404 that the addition of a polyTRIS branch of similar length (entries **7 & 9, 11 & 12**) leads to a
405 decrease in micelle size. A decrease of the aggregation number is also observed as a
406 consequence of the high curvature of the polar head group of each monomer engaged in the
407 micelle.

408 **Comparison between H/F-surfactants.** It has long been shown for surfactants whose
409 hydrophobic tail contains more than 6 perfluorinated carbons linked to a short hydrocarbonated
410 part (methylene groups), that $1 CF_2 \approx 1.5-1.7 CH_2$ ref.^{36, 37} This means that a F_6 -chain is
411 equivalent to roughly a H_{10} one. In our case, since each perfluorocarbon tail is followed by two
412 methylene units, the tail of the F_6 -chain series is therefore equivalent to that of the H_{12} -chain

413 series, as confirmed by the size parameters for H- and F-DendriTACs, which have similar DP_n
414 values and same AB₂ branching type (see entries **3** & **7**). However, smaller assemblies are
415 observed with fluorinated analogues due to the enhanced hydrophobic interaction and stiffness
416 of the fluorocarbon chains that confers them a different packing into the micelle core compared
417 to their hydrocarbon analogues. This is also observed for surfactants endowed with linear polar
418 heads H- and F-TAC surfactants (see entries **14** & **15**). In both linear or dendritic families, N_{ag}
419 is lower for F₆-series than for H₁₂-series due to the bulkiest and rigidity of F-chains that do not
420 allow as much hydrophobic chains in the micelle core as for H-chains.

421 **Comparison between H/F-TAC and H/F-DendriTAC surfactants.** As mentioned above,
422 H₁₂TAC₆ and F₆TAC₇ can be considered to have both comparable hydrophobic contribution of
423 their tail and length of their polyTRIS polar head. However, smaller assemblies are obtained
424 for F₆TAC₇ due to the different molecular packing of fluorinated monomers into the
425 supramolecular construct. Now, if we compare the linear surfactant F₆TAC₇ to its closest
426 dendritic counterpart F₆DiTAC₇ it appears that the structural parameters of the resulting
427 assemblies (R_G , R_H and N_{ag}) are very close. Then, if we extrapolate the comparison and consider
428 F₆TAC₇ as the AB₁ analogue of the F₆-DendriTAC series, it seems that the presence of the
429 central scaffold between the F₆-chain and the polyTRIS head groups attenuates the impact of
430 the branching effect on the micelle size and aggregation number when comparing F₆TAC₇ (AB₁
431 analogue) to F₆DiTAC₇ (AB₂ analogue). However, one can assume that the presence of the two
432 triazole rings and the space between the two oligomeric head groups will influence their
433 respective performances in terms of encapsulation efficiency or as potential nanoreactors.
434 Addition of one supplementary polyTRIS branch to the polar head (from F₆DiTAC₇ to
435 F₆TriTAC₇) induces a decrease in the micelle size and aggregation number, as already
436 commented (entries **7** & **9**). The same tendency is observed for double-tail analogues
437 DiF₆DiTAC₆ and DiF₆TriTAC₈ (entries **11** & **12**). Surprisingly, the introduction of a fourth

438 polyTRIS branch *via* an increase in surfactant generation (from a G_1/AB_2 polar head (entry 7)
439 to a G_1/AB_3 (entry 9) and then to a G_2/AB_2-AB_2 *i.e.* a TetraTAC polar head (entry 10)) cancels
440 out micelle size fluctuations without compensating for N_{ag} variations when moving from
441 G_1/AB_2 to G_1/AB_3 and then to G_2/AB_2-AB_2 monomers. The same trend can be seen with the
442 double-tail surfactants (entries 11, 12 and 13, Figure 5-A, B & C). Again, we can assume that
443 for comparable object size, these different types of assemblies will not offer the same loading
444 capacity for drug delivery or as nanoreactors. For these application types, the high intrinsic
445 variability of the self-assemblies generated by our new family of dendritic surfactants should
446 make H/F-DendriTACs much more versatile platforms than H/F-TACs.

447

448 CONCLUSION

449 In this study, the synthesis of a new dendritic surfactant family called H/F-DendriTAC is
450 described, consisting of either hydrogenated or fluorinated alkyl chains grafted to dendronized
451 hydrophilic oligomers leading to a high structural modularity. All compounds showed a good
452 solubility in water, which allowed their self-assembling study. The aggregation behavior of
453 fifteen surfactants was investigated using small-angle X-ray scattering (SAXS) and dynamic
454 light scattering (DLS) to assess micellar structural parameters, such as their radius of gyration
455 (R_G), volume-weighted hydrodynamic radius (R_H) and aggregation number (N_{ag}). The
456 versatility of the resulting molecular architectures (varying in both the nature, length and
457 number of hydrophobic chains, and number and length of oligomeric polyTRIS polar branches)
458 allows to obtain a large library of micellar aggregates of nanometric size and variable
459 aggregation number. Overall, the high structural versatility of H/F-DendriTAC surfactants,
460 which offers tunable self-assembly behaviors, opens perspectives for a wide range of
461 applications. In ongoing researches, their potential use as nanoreactors for micellar catalysis
462 and as nanocarriers for drug delivery will be investigated.

463

464 Acknowledgements

465 This research was funded by ERANET EuroNanoMed-II program (Project SonoTherag). The
466 authors are grateful to the LaBex ChemiSyst for funding the PhD thesis grant of V. Lacanau
467 (ANR-10-LABX-05-01). We gratefully acknowledge ESRF (European Synchrotron Radiation
468 Facilities at Grenoble, France) for beamtimes on BM29 beamline, and we thank Dr Petra Pernot
469 (BM29) for assistance during SAXS experiments. We also thank Dr Olivier Diat from ICSM
470 (Marcoule-France) for giving us access to the ICSM SAXS instrument during the ESRF
471 shutdown for experiments on F-DendriTACs and his help for SAXS measurements.

472

473 REFERENCES

- 474 (1) Yukuyama, M. N.; Ghisleni, D. D. M.; Pinto, T. J. A.; Bou-Chacra, N. A. Nanoemulsion: process
475 selection and application in cosmetics - a review. *Int. J. Cosmetic Sci.* **2016**, *38* (1), 13-24. DOI:
476 10.1111/ics.12260.
- 477 (2) Sorrenti, A.; Illa, O.; Ortuno, R. M. Amphiphiles in aqueous solution: well beyond a soap bubble.
478 *Chem. Soc. Rev.* **2013**, *42* (21), 8200-8219. DOI: 10.1039/c3cs60151j.
- 479 (3) Schramm, L.; Stasiuk, E.; Marangoni, G. Surfactants and their Applications. *Annu. Rep. Prog. Chem.,*
480 *Sect. C: Phys. Chem.* **2003**, *99*, 3-48. DOI: 10.1039/B208499F.
- 481 (4) Malmsten, M. *Surfactants and polymers in drug delivery*; 2002.
- 482 (5) Tadros, T. Food Surfactants. In *Encyclopedia of Colloid and Interface Science*, Tadros, T. Ed.; Springer
483 Berlin Heidelberg, 2013; pp 555-556.
- 484 (6) Parshad, B.; Prasad, S.; Bhatia, S.; Mittal, A.; Pan, Y.; Mishra, P. K.; Sharma, S. K.; Fruk, L. Non-ionic
485 small amphiphile based nanostructures for biomedical applications. *RSC Adv.* **2020**, *10* (69), 42098-
486 42115. DOI: 10.1039/D0RA08092F.
- 487 (7) Desgranges, S.; Lorton, O.; Gui-Levy, L.; Guillemin, P.; Celicanin, Z.; Hyacinthe, J. N.; Breguet, R.;
488 Crowe, L. A.; Becker, C. D.; Soulie, M.; et al. Micron-sized PFOB liquid core droplets stabilized with
489 tailored-made perfluorinated surfactants as a new class of endovascular sono-sensitizers for focused
490 ultrasound thermotherapy. *J. Mater. Chem. B* **2019**, *7* (6), 927-939. DOI: 10.1039/c8tb01491d.
- 491 (8) Astafyeva, K.; Somaglino, L.; Desgranges, S.; Berti, R.; Patinote, C.; Langevin, D.; Lazeyras, F.;
492 Salomir, R.; Polidori, A.; Contino-Pépin, C.; et al. Perfluorocarbon nanodroplets stabilized by fluorinated
493 surfactants: characterization and potentiality as theranostic agents. *J. Mater. Chem. B* **2015**, *3* (14),
494 2892-2907. DOI: 10.1039/c4tb01578a.
- 495 (9) Contino-Pépin, C.; Parat, A.; Patinote, C.; Roscoe, W. A.; Karlik, S. J.; Pucci, B. Thalidomide
496 Derivatives for the Treatment of Neuroinflammation. *ChemMedChem* **2010**, *5* (12), 2057-2064. DOI:
497 10.1002/cmdc.201000326.
- 498 (10) Jasseron, S.; Contino-Pépin, C.; Maurizis, J. C.; Rapp, M.; Pucci, B. In vitro and in vivo evaluations
499 of THAM derived telomers bearing RGD and Ara-C for tumour neovasculature targeting. *Eur. J. Med.*
500 *Chem.* **2003**, *38* (9), 825-836. DOI: 10.1016/S0223-5234(03)00150-8.
- 501 (11) Rosen, B. M.; Wilson, C. J.; Wilson, D. A.; Peterca, M.; Imam, M. R.; Percec, V. Dendron-Mediated
502 Self-Assembly, Disassembly, and Self-Organization of Complex Systems. *Chem. Rev.* **2009**, *109* (11),
503 6275-6540. DOI: 10.1021/cr900157q.

504 (12) Apartsin, E.; Caminade, A.-M. Supramolecular Self-Associations of Amphiphilic Dendrons and Their
505 Properties. *Chem. Eur. J.* **2021**, *27* (72), 17976-17998. DOI: 10.1002/chem.202102589.

506 (13) Thota, B. N. S.; Urner, L. H.; Haag, R. Supramolecular Architectures of Dendritic Amphiphiles in
507 Water. *Chem. Rev.* **2016**, *116* (4), 2079-2102. DOI: 10.1021/acs.chemrev.5b00417.

508 (14) Singh, A. K.; Thota, B. N. S.; Schade, B.; Achazi, K.; Khan, A.; Böttcher, C.; Sharma, S. K.; Haag, R.
509 Aggregation Behavior of Non-ionic Twinned Amphiphiles and Their Application as Biomedical
510 Nanocarriers. *Chem Asian J* **2017**, *12* (14), 1796-1806. DOI: 10.1002/asia.201700450.

511 (15) Rashmi, R.; Hasheminejad, H.; Herziger, S.; Mirzaalipour, A.; Singh, A. K.; Netz, R. R.; Böttcher, C.;
512 Makki, H.; Sharma, S. K.; Haag, R. Supramolecular Engineering of Alkylated, Fluorinated, and Mixed
513 Amphiphiles. *Macromol Rapid Commun* **2022**, *43* (8), 2100914. DOI: 10.1002/marc.202100914.

514 (16) Roy, R.; Shiao, T. C. Glyconanosynthons as powerful scaffolds and building blocks for the rapid
515 construction of multifaceted, dense and chiral dendrimers. *Chem. Soc. Rev.* **2015**, *44* (12), 3924-3941.
516 DOI: 10.1039/c4cs00359d.

517 (17) Teulère, C.; Nicolaÿ, R. Synthesis of molecular brushes by telomerization. *Polym. Chem.* **2017**, *8*
518 (34), 5220-5227. DOI: 10.1039/c7py00875a.

519 (18) Chabre, Y. M.; Contino-Pépin, C.; Placide, V.; Shiao, T. C.; Roy, R. Expeditive Synthesis of
520 Glycodendrimer Scaffolds Based on Versatile TRIS and Mannoside Derivatives. *J. Org. Chem.* **2008**, *73*
521 (14), 5602-5605. DOI: 10.1021/jo8008935.

522 (19) Li, L.; Zahner, D.; Su, Y.; Gruen, C.; Davidson, G.; Levkin, P. A. A biomimetic lipid library for gene
523 delivery through thiol-yne click chemistry. *Biomaterials* **2012**, *33* (32), 8160-8166. DOI:
524 10.1016/j.biomaterials.2012.07.044.

525 (20) Berne, D.; Ladmiral, V.; Leclerc, E.; Caillol, S. Thia-Michael Reaction: The Route to Promising
526 Covalent Adaptable Networks. *Polymers* **2022**, *14* (20). DOI: 10.3390/polym14204457 From NLM.

527 (21) Boncel, S.; Mączka, M.; Walczak, K. Z. Michael versus retro-Michael reaction in the regioselective
528 synthesis of N-1 and N-3 uracil adducts. *Tetrahedron* **2010**, *66* (43), 8450-8457. DOI:
529 10.1016/j.tet.2010.08.059.

530 (22) Rostovtsev, V. V.; Green, L. G.; Fokin, V. V.; Sharpless, K. B. A Stepwise Huisgen Cycloaddition
531 Process: Copper(I)-Catalyzed Regioselective "Ligation" of Azides and Terminal Alkynes. *Angew. Chem.*
532 *Int. Ed.* **2002**, *41* (14), 2596-2599. DOI: 10.1002/1521-3773.

533 (23) Tornøe, C. W.; Christensen, C.; Meldal, M. Peptidotriazoles on Solid Phase: [1,2,3]-Triazoles by
534 Regiospecific Copper(I)-Catalyzed 1,3-Dipolar Cycloadditions of Terminal Alkynes to Azides. *J. Org.*
535 *Chem.* **2002**, *67* (9), 3057-3064. DOI: 10.1021/jo011148j.

536 (24) Svergun, D. I. Determination of the regularization parameter in indirect-transform methods using
537 perceptual criteria. *J Appl Crystallogr* **1992**, *25* (4), 495-503. DOI: 10.1107/S0021889892001663.

538 (25) Durchschlag, H.; Zipper, P. Calculation of Partial Specific Volumes and Other Volumetric of
539 Detergents and Lipids. *Jorn. Com. Esp. Deterg.* **1995**, *29*, 275-292.

540 (26) Linke, D. Chapter 34 Detergents: An Overview. In *Methods in Enzymology*, Burgess, R. R.,
541 Deutscher, M. P. Eds.; Vol. 463; Academic Press, 2009; pp 603-617.

542 (27) Oliver, R. C.; Lipfert, J.; Fox, D. A.; Lo, R. H.; Doniach, S.; Columbus, L. Dependence of Micelle Size
543 and Shape on Detergent Alkyl Chain Length and Head Group. *PLoS One* **2013**, *8* (5), e62488. DOI:
544 10.1371/journal.pone.0062488.

545 (28) Lipfert, J.; Columbus, L.; Chu, V. B.; Lesley, S. A.; Doniach, S. Size and Shape of Detergent Micelles
546 Determined by Small-Angle X-ray Scattering. *J. Phys. Chem. B* **2007**, *111* (43), 12427-12438. DOI:
547 10.1021/jp073016l.

548 (29) Israelachvili, J. N.; Mitchell, D. J.; Ninham, B. W. Theory of self-assembly of hydrocarbon
549 amphiphiles into micelles and bilayers. *J. Chem. Soc., Faraday Trans. 2* **1976**, *72* (0), 1525-1568. DOI:
550 10.1039/F29767201525.

551 (30) Leung, S. C. E.; Wanninayake, D.; Chen, D.; Nguyen, N.-T.; Li, Q. Physicochemical properties and
552 interactions of perfluoroalkyl substances (PFAS) - Challenges and opportunities in sensing and
553 remediation. *Sci. Total Environ.* **2023**, *905*, 166764. DOI: 10.1016/j.scitotenv.2023.166764.

554 (31) Krafft, M. P.; Riess, J. G. Chemistry, Physical Chemistry, and Uses of Molecular
555 Fluorocarbon-Hydrocarbon Diblocks, Triblocks, and Related Compounds—Unique "Apolar"

556 Components for Self-Assembled Colloid and Interface Engineering. *Chem. Rev.* **2009**, *109* (5), 1714-
557 1792. DOI: 10.1021/cr800260k.
558 (32) Hasegawa, T. Physicochemical Nature of Perfluoroalkyl Compounds Induced by Fluorine. *The*
559 *Chemical Record* **2017**, *17* (10), 903-917. DOI: 10.1002/tcr.201700018.
560 (33) Maibaum, L.; Dinner, A. R.; Chandler, D. Micelle Formation and the Hydrophobic Effect. *J. Phys.*
561 *Chem. B* **2004**, *108* (21), 6778-6781. DOI: 10.1021/jp037487t.
562 (34) Nagarajan, R. Molecular Packing Parameter and Surfactant Self-Assembly: The Neglected Role of
563 the Surfactant Tail. *Langmuir* **2002**, *18* (1), 31-38. DOI: 10.1021/la010831y.
564 (35) Tanford, C. *The hydrophobic effect: formation of micelles and biological membranes 2d ed*; J.
565 Wiley., 1980.
566 (36) Sadtler, V. M.; Giulieri, F.; Krafft, M. P.; Riess, J. G. Micellization and Adsorption of Fluorinated
567 Amphiphiles: Questioning the $1\text{CF}_2 \approx 1.5\text{CH}_2$ Rule. *Chem. Eur. J.* **1998**, *4* (10), 1952-1956. DOI:
568 10.1002/(SICI)1521-3765(19981002)4:10<1952::AID-CHEM1952>3.0.CO;2-V.
569 (37) Shinoda, K.; Hato, M.; Hayashi, T. Physicochemical properties of aqueous solutions of fluorinated
570 surfactants. *J. Phys. Chem.* **1972**, *76* (6), 909-914. DOI: 10.1021/j100650a021.

571

572